Pressure effect due to wind interference between mid-rise and high-rise buildings

Pressure effects due to wind interference between mid-rise and high-rise buildings

A.J. Bronkhorst [a,b], C.P.W. Geurts [a,b], B. Blocken [b] and C.A. van Bentum [a]

[a] *TNO, Delft, the Netherlands*
[b] *Eindhoven University of Technology, Department of Architecture, Building and Planning, Eindhoven, the Netherlands, a.j.bronkhorst@tue.nl*

1 INTRODUCTION

Wind loads on cladding of buildings are likely to be influenced by the presence of nearby tall buildings. The influence of neighboring buildings on global wind loads has been researched extensively in the 80's and 90's. Studies by Taniike (1991) and Khanduri (1997) concluded that the influence of interfering buildings with similar or larger heights than the reference building could lead to an increase in global wind loads of 70-80%, but judged the influence of smaller buildings on the global loads insignificant. Studies on the influence of a high-rise building on surrounding buildings mention a factor two to three increase in local peak loads [Stathopoulos (1984), Surry and Malais (1982)]. Recently Kim et al (2011) studied the influence of a mid-rise building on the local loads experienced by the facades of a high-rise building; they found an increase in minimum peak suction of approximately 15%.
From a wind tunnel measurement (Figure 1) on a 165 m high tower in Rotterdam, the Netherlands, a characteristic value for the peak suction of -5255 N/m^2 was calculated at tap (1) at a wind angle of 210º (Geurts et al, 2006). This value is over a factor three higher than the value found when applying the Dutch Code (NEN6702, 2001) at this height (105 m full scale). Figure 1(b) illustrates that the building 22 m upstream is likely to have an influence on this extreme peak pressure.
This paper aims at understanding the wind effects of a mid-rise building on the pressure distribution of a nearby high-rise building.

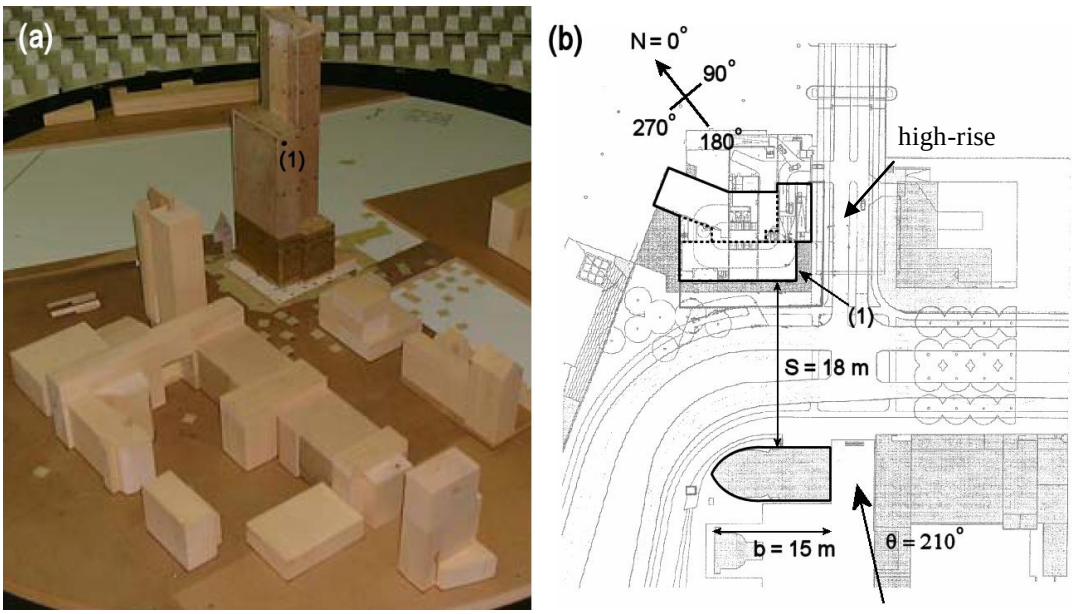

Figure 1. (a) Wind tunnel model of the high-rise building and surroundings in Rotterdam, (b) top view of the 165 m high-rise and interfering building (S/b = 1.2) and (c) histograms of minimum pressure coefficients for tap positions (1) and (2) referenced to the mean free stream dynamic pressure at roof height.

2 DESCRIPTION WIND TUNNEL TEST

Wind tunnel experiments have been carried out in the open circuit atmospheric boundary layer (ABL) wind tunnel of TNO Built Environment and Geosciences in the Netherlands, illustrated in Figure 2. It has a working section of approximately 13.5 m in length; the test section has a 3 m width and 2 m height.

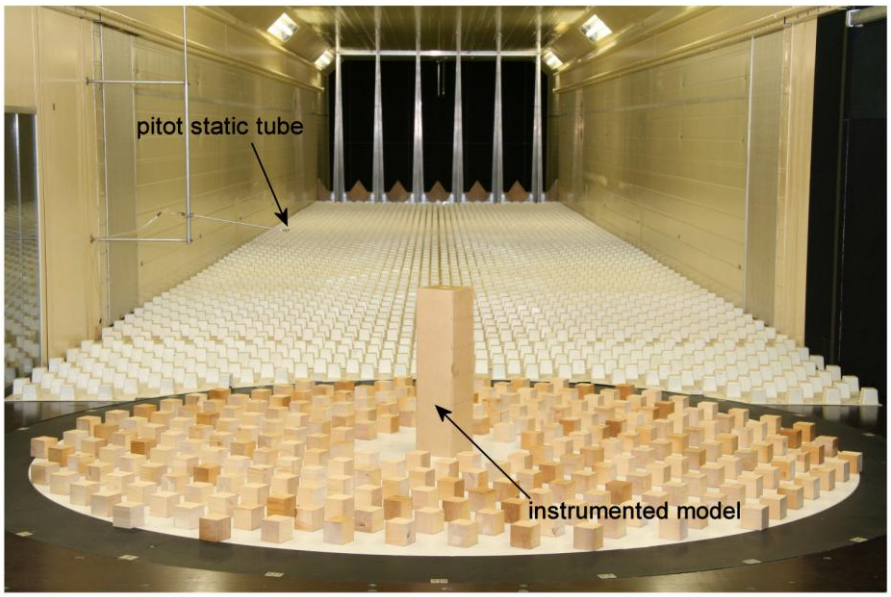

Figure 2. The isolated test configuration in the wind tunnel of TNO.

The boundary layer applied in this study was developed using 6 spires and 50 mm cubic roughness elements equally spaced over the length of the test section. The roughness elements extended onto the turn table, as illustrated in Figure 2, to prevent the development of an internal boundary layer. This particular configuration was chosen since it represents a suburban fetch. This corresponds to the typical conditions found in practice in the Netherlands when new high rise buildings are being developed.

The three velocity components of the wind tunnel boundary layer have been measured with a Dantec Dynamics two-component hot wire anemometer in two separate runs. Mean flow velocities have been determined from measurements sampled with 68 Hz for 60 s, a sampling rate of 500 Hz and sampling time of 8.2 s were applied for the determination of the turbulence intensities and spectral properties. Measurements have been made above the centre of the turntable without building models present.

For an accurate determination of the roughness length z_0 and displacement height d, the friction velocity has been determined with $u_* = \sqrt{-\overline{u'w'}} = 1.13$ (Roth, 1993), in which $\overline{u'w'}$ is the Reynolds stress near the wall. A linear fit through a rearranged logarithmic law results in wind tunnel values of z_0 = 0.0032 m and d = 0.018 m, the velocity profile is illustrated in Figure 3(a). The Jensen number for this test configuration is 150. A geometrical scaling of 250 results in full scale values z_0 = 0.8 m and d = 4.6 m.

Both the turbulence intensities and the power spectral densities were determined using ensemble averaging over 4 ensembles with a length of approximately 2 s. Between 0.1 m and 0.5 m height the turbulence intensities, non-dimensionalized by the friction velocity, can be considered constant because the coefficient of variation is smaller than 0.1. For this region the mean intensity values are σ_u/u_* = 2.0, σ_v/u_* = 1.7 and σ_w/u_* = 1.4. Table 1 provides values and ranges (obtained at different heights) from different full scale atmospheric boundary layer studies over rough terrain in neutral conditions. Although in this study, σ_u/u_* is small, the wind tunnel values fit within the ranges found in these studies. The turbulence intensity profiles are illustrated in Figure 3(b).

Table 1. Full-scale values for the fraction of velocity standard deviation values σ_u, σ_v and σ_w divided by the friction velocity u_*.

Source	σ_u/u_*	σ_v/u_*	σ_w/u_*
Panofksy & Dutton (1984)	2.5	2.0	1.25
Duchene-Marullaz (1997)	2.0	1.5	1.0
Roth (1993)	2.1-2.7	1.2-2.3	1.0-1.7
Rotach (1995)	1.2-1.7	1.1-1.7	0.7-1.3
Geurts (1997)	2.4	1.9	1.4

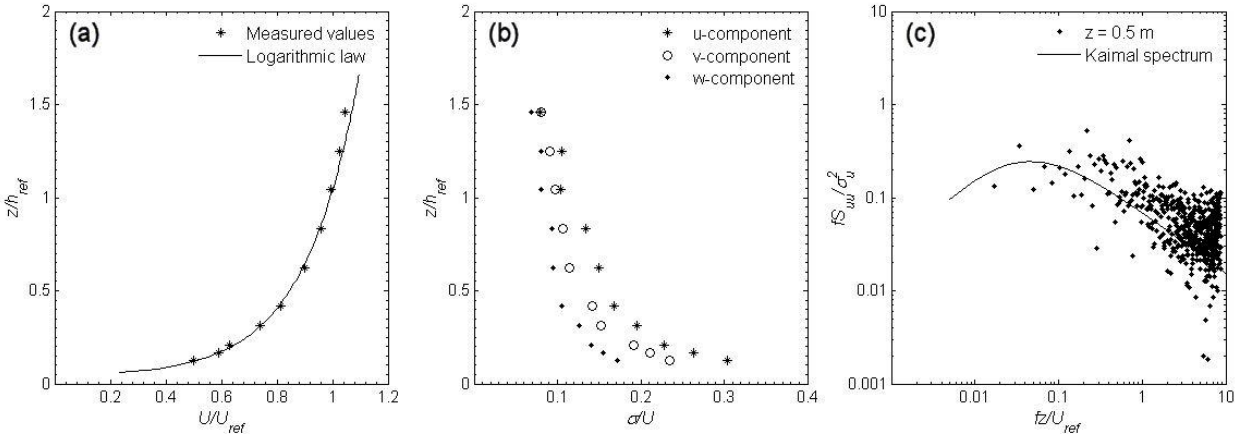

Figure 3. Simulated wind characteristics: (a) mean velocity profile U/U_{ref} , (b) turbulence intensity profiles I_u, I_v and I_w and (c) the longitudinal power density spectrum fS_{uu}/σ_u^2.

Power spectra of the turbulence components were computed with the Fast Fourier Transform. The longitudinal non-dimensional spectrum versus the reduced frequency is illustrated in Figure 3(c) for a height of z = 0.5 m.

The reference model is a wooden square cylinder with a height of h = 0.48 m and both sides b = 0.12 m. The interfering model, also made of wood, has a height of 0.24 m and the same horizontal dimensions as the reference model. Measurements were performed on the isolated configuration and three tandem configurations [as illustrated in Figure 4(b)]. Both the influence of a square and circular shape of the interfering building is investigated. Twenty-four wind directions were measured for each configuration.

The reference model is instrumented with pressure taps at 86 locations. The taps are distributed as illustrated in Figure 4, 38 pressure taps on the front and rear face and 10 taps on the top face. After one measurement run the model was rotated 90 degrees and a second run was performed for the same configuration.

The fluctuating pressures acting at the 1.1 mm diameter pressure taps were measured with a sampling rate of 400 Hz for a period of approximately 20.5 seconds. The distortion of the measured pressures due to the tube length was corrected for with transfer functions.

During pressure measurements the undisturbed static and dynamic pressure and mean wind speed in the wind tunnel, U_{ref} = 14.2 m/s, were measured with a pitot-static tube positioned at model roof height (h_{ref} = 0.48 m), approximately 2.6 m in front of the model and 0.7 m to the side.

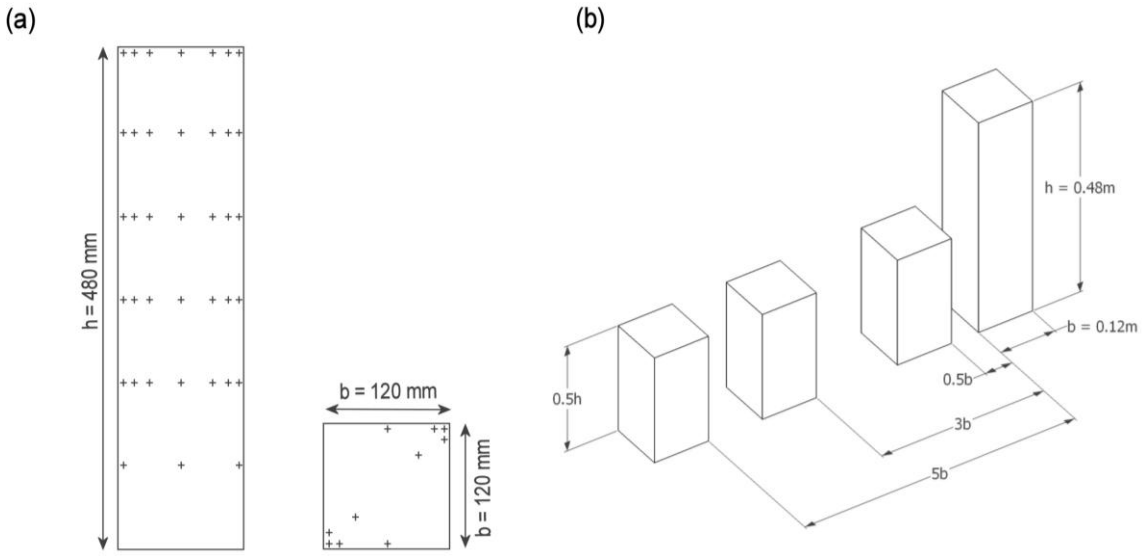

Figure 4. (a) Pressure tap distribution on the side faces and top face of the instrumented building model, (b) 4 tandem configuration positions measured in the wind tunnel (the circular shaped interfering building is not illustrated).

The measured pressures are converted into pressure coefficients using:

$$C_{\bar{p}} = \frac{\bar{p}}{\frac{1}{2}\rho U_{ref}^2} \quad \text{and} \quad C_{\sigma_p} = \frac{\sigma_p}{\frac{1}{2}\rho U_{ref}^2}.$$

In which $\bar{p}$ and σ_p are the mean and standard deviation of the measured pressure signal.

3 RESULTS AND DISCUSSION

A mean and standard deviation pressure coefficient were determined for twenty-four wind directions at all pressure tap positions. For each tap position the minimum, over all wind directions, of the mean pressure coefficients was determined; the maximum standard deviation was obtained with the same method. Figure 5 presents the minimum mean (a) and maximum standard deviation (b) pressure coefficient contours. The contours on the front (A), side (B) and rear (C) face are illustrated for the rectangular and circular interfering building cases at $S = 0.5b$. For the isolated case, the pressure coefficient contours on the four faces are similar when all wind directions are considered; therefore only one of the pressure coefficient contours is illustrated in figures 5(a) and (b). Regions on the building with a significant effect in minimum mean pressure and maximum standard deviation pressure are indicated with the symbols ■, ● and ▲. Table 2 gives the minimum mean and maximum standard deviation coefficients measured at these locations, as well as the wind directions where these values were measured. The next paragraph will describe some characteristics of the three pressure effects encountered on the faces of the building model.

3.1 *Pressure effect characteristics*

On face A at the location specified with the symbol ■, both the square and circular interfering building cause an increase in minimum mean pressure coefficient of approximately 19%. This increase is observed at a 285º wind angle for the square interfering building and a 270º wind angle for the circular interfering building. The maximum standard deviation coefficient does not increase; however, the wind angle where this maximum is measured has changed from 300º to 285º. In case of a square interfering building the largest mean and fluctuating pressure effects occur at the same wind angle. These effects are the result of the flow phenomenon known as channeling [(Blocken et al, 2007), (Lam et al, 2008)].

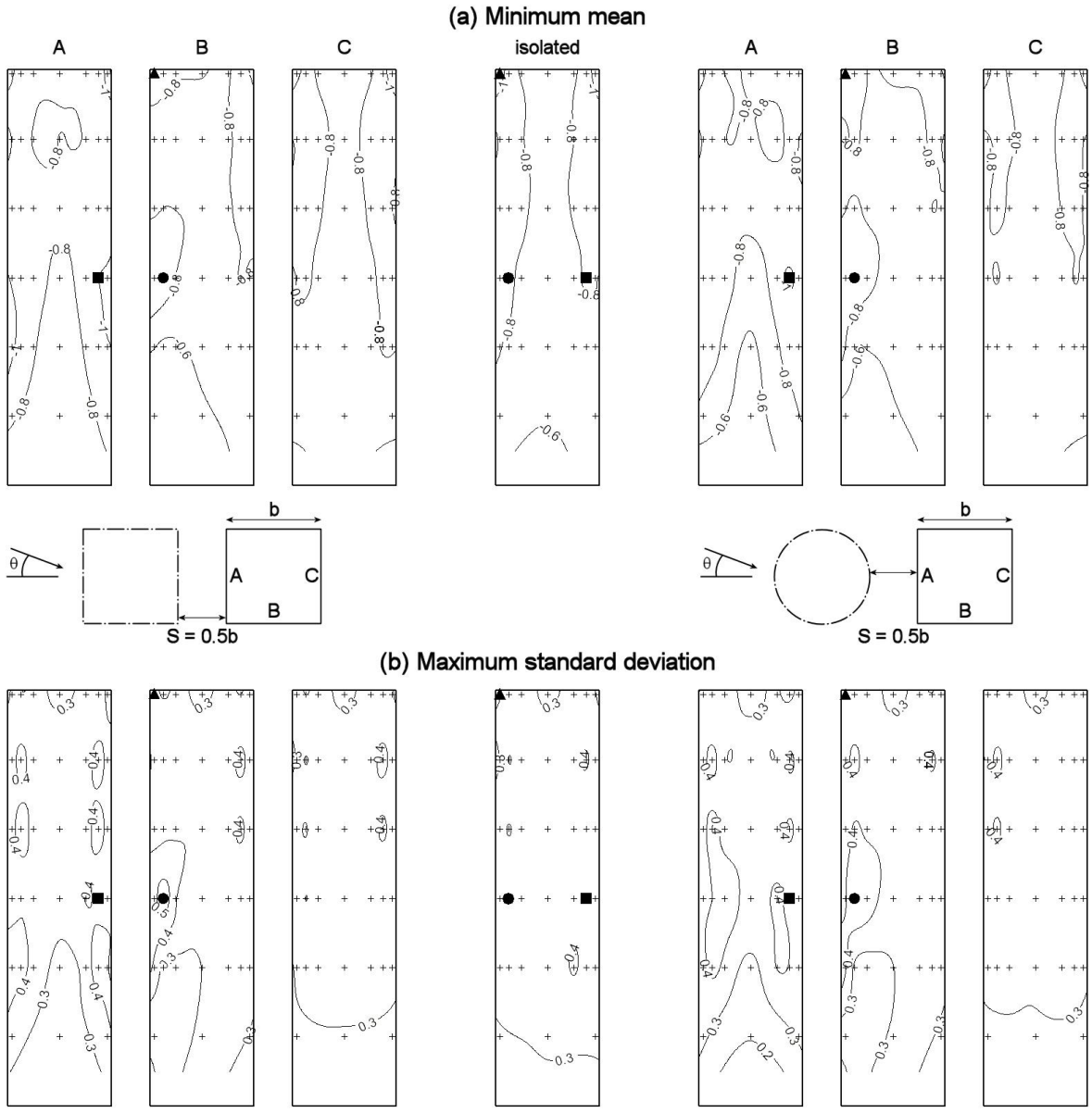

Figure 5. Pressure coefficient contours of (a) minimum mean and (b) maximum standard deviation values determined on the front (A), side (B) and rear (C) faces of the high-rise building model over 24 wind angles. The isolated case (centre) and two interfering cases (square cylinder left and circular cylinder right) with $S = 0.5b$ are presented. The symbols ■ and ● specify locations where a significant increase in minimum mean and maximum standard deviation is observed; a reduction in minimum mean and maximum standard deviation is observed at ▲.

Table 2. Pressure coefficient values for the specified locations in Figure 5. For each position the minimum mean and maximum standard deviation over all wind directions are provided, plus the wind angle at which this minimum or maximum was determined.

Case	***min*** $C_{p,mean}$	θ	***max*** $C_{p,std}$	θ
Isolated (■)	-0.85	285°	0.39	300°
Square-square (■)	-1.00	285°	0.39	285°
Circle-square (■)	-1.01	270°	0.38	285°
Isolated (●)	-0.84	345°	0.37	330°
Square-square (●)	-0.92	0°	0.55	345°
Circle-square (●)	-0.90	0°	0.47	345°
Isolated (▲)	-1.08	345°	0.41	345°
Square-square (▲)	-0.89	345°	0.34	330°
Circle-square (▲)	-0.95	345°	0.36	330°

This phenomenon also occurs at the same position on the other side of face A at wind angles between approximately 60º and 90º. Figure 6(a) illustrates the configuration and the region of influence. The influence of a mid-rise building on a high-rise building due to channeling is limited (smaller than 20%). More significant effects were observed by Bronkhorst et al (2010) and Kim et al (2011) for buildings of equal height. Bronkhorst et al (2010) determined increases of approximately 60% in minimum mean and 40% in maximum standard deviation; Kim et al (2011) describe a 40% increase in minimum peak pressure coefficient.

On face B at half the building height (●) the square mid-rise building causes a 10% increase in minimum mean and a 49% increase in maximum standard deviation coefficient. At the same position, the circular building produces an increase in minimum mean pressure coefficient of 7% and a 27% increase in maximum standard deviation pressure coefficient. These effects occur at wind angles of 0º and 345º (table 2). The location of the effect and the wind angles at which it was measured, illustrated in figure 6(b), indicate that the interference effect is related to the shear layer separating from the roof of the mid-rise building.

At the top corner of face B (▲) a reduction in minimum mean and maximum standard deviation pressure coefficient is observed. A square-shaped interfering building reduces minimum mean with 18% and maximum standard deviation with 17%; the circular building reduces both minimum mean and maximum standard deviation coefficient with 12%. The minimum mean pressure coefficient occurs for all cases at a wind angle of 345º. The interfering building changes the wind angle at which the maximum standard deviation is determined from 345º to 330º.

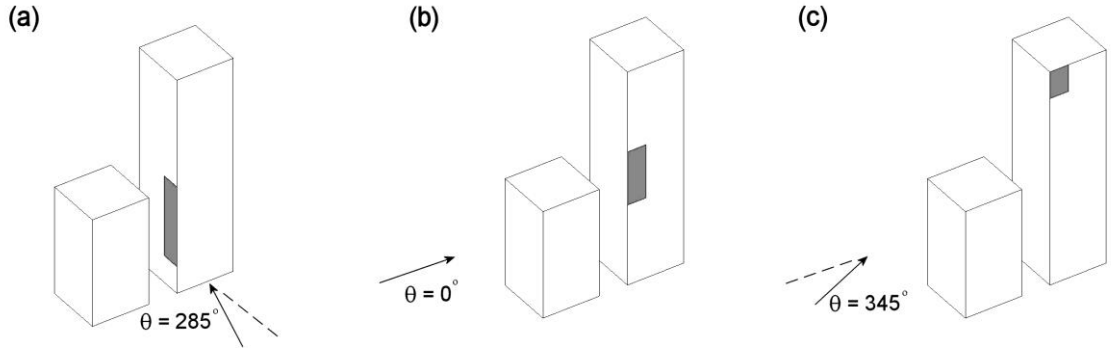

Figure 6. Illustrations of the identified cases with effects on mean and standard deviation pressure coefficient: (a) channelling effect, (b) shear layer impingement effect and (c) corner pressure reduction effect. The grey zones indicated the region where the pressure effects are observed. The circular-shaped interfering building is not illustrated.

3.2 *Influence of separation distance*

The influence of the non-dimensional separation distance *S/b* on the minimum mean and maximum standard deviation pressure coefficient is illustrated in the graphs of Figure 7(a) and (b).

The first graph of figure 7(a) and 7(b) show the influence of *S/b* on the minimum mean and maximum standard deviation pressure determined at the position indicated with ■. These pressure effects, related to the channeling phenomenon, are only significant at a separation distance *S/b* = 0.5. For separation distance *S/b* = 3 and *S/b* = 5 the mean and standard deviation pressure coefficient are similar to the isolated case coefficients. Both the square and circular interfering building have a comparable influence on the mean as well as the standard deviation pressure coefficient at the specified location (■) on the building.

The second graph of figure 7(a) and (b) show the influence of separation distance on the minimum mean and maximum standard deviation pressure coefficient at position ●. For separation distances *S/b* = 3 and *S/b* = 5, the minimum mean or maximum standard deviation pressure coefficient are comparable to the isolated case. At a separation distance of *S/b* = 0.5, the square interfering building has a 17% larger influence than the circular interfering building.

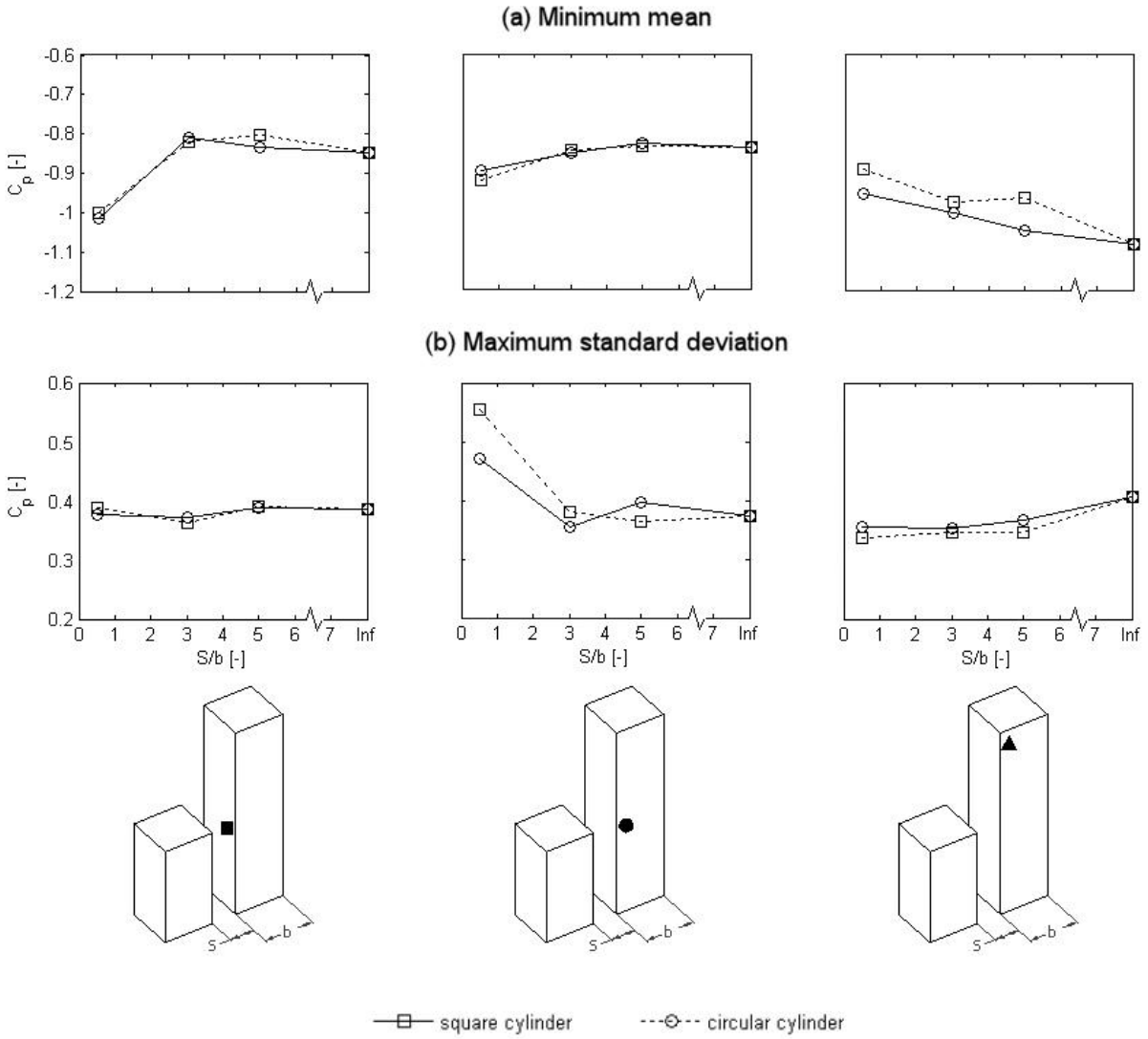

Figure 7. Ratio of separation distance *S* and model width *b* versus the minimum mean (a) and maximum standard deviation (b) pressure coefficient values. The first column of graphs illustrates the channelling effect (■), the second column the shear layer impingement effect (●) and the third column the pressure alleviation effect (▲).

The influence of separation distance on the minimum mean and maximum standard deviation pressure in the top corner of the high-rise building model is illustrated in the third graph of figure 7(a) and (b). Both the mean and the fluctuating component of the pressure show the largest reduction at a separation distance of $S/b = 0.5$. In contrast to the previous two effects, the corner pressure is still influenced at separation distances of $S/b = 3$ and $S/b = 5$. The square interfering building has a slightly larger influence than the circular building.

4 CONCLUSION

Based on the mean and standard deviation pressure distribution, three interference effects were determined: a channeling effect, a shear layer impingement effect and a pressure alleviation effect. For the first two effects increases in minimum mean and maximum standard deviation pressure coefficient were observed at half the height of the high-rise building. A reduction in both mean and standard deviation pressure coefficient were determined for the third effect, which occurs at the top corner of both side faces.

The adverse effects of the mid-rise building on the mean and standard deviation pressure distribution are significant for a separation distance of $S/b = 0.5$. For separation distance $S/b > 3$ the investigated adverse effects are considered insignificant with a maximum influence in both mean and standard deviation coefficient of less than 10%. For separation distances of at least up to $S/b = 5$, the mid-rise building has a favorable effect on the pressure encountered in the top corner on the side face of the disturbed high-rise building. Both the mean and standard deviation pressure coefficient are reduced by the interfering building, either square of circular.

Overall, the square building has a larger influence than the circular building. In case of the shear layer impingement effect, the square interfering building generates a larger standard deviation pressure coefficient. The square interfering building also causes a larger reduction in both mean and standard deviation pressure coefficient at the top corner of the high-rise building.

Future analysis of the flow field will provide for a better understanding of the origin of the increases and alleviations in the mean and fluctuating components of the measured pressures.

5 REFERENCES

Blocken B., Carmeliet, J., Stathopoulos, T., 2007. CFD evaluation of wind speed conditions in passages between parallel buildings – effect of wall-function roughness modifications for the atmospheric boundary layer flow, J. Wind Eng. Ind. Aerodyn. 95, 941-962.

Bronkhorst, A.J., Geurts, C.P.W., Blocken, B., Van Bentum, C.A., 2010, Adverse local wind effects on neighboring buildings, Recent advances in research on environmental effects on buildings and people, 167-177.

Duchene-Marullaz, Ph., 1979, Effect of high roughness on the characteristics of turbulence in cases of strong wind, Proc. of the 5th Conference on Wind Engineering, Fort Collins, 179-193.

Geurts, C.P.W., Visser, G.Th., van Bentum, C.A., 2006. Bepaling van de ontwerp windbelastingen op de fundering en de locale windbelasting op gevels en dakonderdelen van de geprojecteerde Maastoren in Rotterdam, TNO report 2006-A-R0059/B.

Geurts, C.P.W., 1997. Wind-induced pressure fluctuations on building facades, PhD thesis, Eindhoven University of Technology.

Khanduri, A.C., 1997. Wind-induced interference effects on buildings: integrating experimental and computerized approaches, PhD thesis, Concordia University.

Kim, W., Tamura, Y., Yoshida, A., 2011. Interference effects on local peak pressures between two buildings, J. Wind Eng. Ind. Aerodyn, 99, 584-600.

Lam K.M., Leung, M.Y.H., Zhao, J.G., 2008, Interference effects on wind loading of a row of closely spaced tall buildings, J. Wind Eng. Ind. Aerodyn. 96, 562-583.

NEN6702 (2001), Technical principles for building structures – TGB 1990 – Loadings and deformations, NEN Norm committee 351001, Delft.

Panofsky, H.A., Dutton, J.A., 1984. Atmospheric Turbulence, models and methods for engineering applications, Wiley International, 359 p.

Roth, M., 1993, Turbulent transfer relationships over an urban surface. II: Integral statistics, Q.J.R. Meteorol. Soc., 1105-1120.

Rotach, M.W., 1995. Profiles of turbulence statistics in and above an urban street canyon, Atmospheric Environment, vol. 29, no. 13, 1473-1486.

Stathopoulos, T., 1984. Adverse wind loads on low buildings due to buffeting, J. Struct. Eng., ASCE, 110(10), 2374-2392.

Surry, D., Malais, W., 1982. Adverse local wind loads induced by adjacent building, J. Struct. Eng., ASCE, 108, 2263-2278.

Taniike, Y., 1992. Interference mechanism for enhanced wind forces on neighbouring tall buildings, J. Wind Eng. Ind. Aerodyn. 41-44, 1073-1083.